Organic Cages

DOI: 10.1002/anie.201202849

Porous Organic Alloys**

*Tom Hasell, Samantha Y. Chong, Marc Schmidtmann, Dave J. Adams, and Andrew I. Cooper**

Multicomponent molecular crystals, or cocrystals,[1] are important in the pharmaceutical industry and as functional materials. However, while two-component organic cocrystals are common, examples comprising three or more different molecules are comparatively rare.[2] By contrast, the use of directional intermolecular bond-forming reactions renders such modularity possible, and this has fuelled tremendous interest in crystalline networks such as metal–organic frameworks (MOFs).[3] For example, so-called "multivariate MOFs" (MTV-MOFs) comprise mixtures of isostructural organic linkers that are cocrystallized into the well-known MOF-5 architecture in a broadly modular, "Lego-like" fashion.[4] That is possible because the coordination bonds between the organic struts and the metal secondary building units (SBUs) dominate the crystal formation energy. Such exquisite programmed modularity has not yet been achieved with molecular organic crystals, despite elegant supramolecular approaches.[5] Despite striking counter-examples,[6] molecular crystals are not typically dominated by a single, highly directional bonding motif. Hence, discrete elements in molecular cocrystals cannot usually be substituted without causing fundamental changes to the crystal packing. It remains very challenging, therefore, to create modular, multicomponent molecular organic crystals in a programmed way.

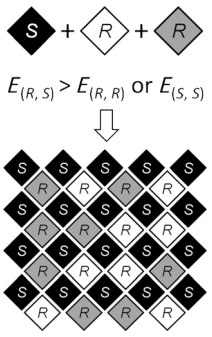

Scheme 1. Design principle for preparing multicomponent systems. *E* is the crystal formation energy.

Here we show that cagelike organic molecules[7] have a robust crystal packing that persists over a wide range of chemical compositions. This can be exploited to generate ternary cocrystals in a modular strategy without the formation of intermolecular bonds. One cage module, **CC1**, is ordered on 50% of the lattice positions with respect to two other modules, **CC3** and **CC4**, that are disordered across the other 50% of sites, forming a solid solution (Scheme 1). There is a linear relationship between relative module composition and the lattice parameters of the cocrystals, in agreement with Vegard's law which is more commonly associated with inorganic alloys and salts.[8] Unlike other tercrystals,[2h] the materials are permanently, measurably porous, and the porosity can be tuned systematically by varying the relative proportions of the modules, thus producing the first truly porous "organic alloys".

Our strategy builds on previous work where we showed that chiral interactions dominate the crystal packing for intrinsically porous imine cage molecules which have permanent, prefabricated cavities.[7b] For example, a homochiral cage, **CC3**-*R*, has a strong energetic preference to crystallize with its *S* enantiomer, **CC3**-*S*, as rationalized by crystal structure prediction calculations[7b] and by density functional theory calculations that showed that opposite cage enantiomers interact more strongly.[9] We also showed that a racemic cage molecule, **CC1**, forms a binary 1:1 porous molecular cocrystal with homochiral **CC3**-*R*. In this case, **CC1** exists in solution as a mixture of interconvertible *R* and *S* enantiomers, yet the resulting cocrystal with **CC3**-*R* contains only the *S* form of **CC1**. As such, the chirality of **CC1** is resolved by cocrystallization with **CC3**-*R*. Hence, these particular isostructural imine cages have a strong tendency to form heterochiral window-to-window pairings in the solid state, and this suggested to us a design principle for preparing more complex, multicomponent systems (Scheme 1).

We use this principle here to assemble ternary cocrystals of three separate cage modules, **CC1**, **CC3**, and **CC4** (Figure 1a). All three cage molecules have tetrahedral symmetry and include four windows that are large enough to be penetrated by small guests.[10] The three modules differ only in terms of functionality on the six vertices of the broadly octahedral-shaped cage (ethane for **CC1**, cyclohexane for **CC3**, and cyclopentane for **CC4**). All three molecules are soluble in common organic solvents and hence cocrystals can be prepared using standard, non-reactive crystallization techniques. A range of ternary compositions was studied using dichloromethane as the crystallization solvent. The materials were prepared according to the design shown in Scheme 1: that is, we targeted an overall 1:1 ratio of *R*:*S* enantiomers, varying the relative mole fraction of the two *R* enantiomers, **CC3**-*R* and **CC4**-*R*, from 0 to 1 (i.e., **CC1**·**CC3**$_n$**CC4**$_{1-n}$, $0 < n < 1$). It should be noted that **CC1** is racemic, but we hypothesized, by analogy with the binary **CC1**-*S*/**CC3**-*R* cocrystal,[7b] that **CC1** would be resolved to its *S* enantiomer in all of the compositions. The cages are molecularly soluble, and therefore the actual ratio incorporated in the crystals could be determined simply by ^{1}H NMR spectroscopy. The relative proportions of the cages incorporated in the crystals were found to agree with the proportions added to the various crystallization solutions (see Figure S1 in

[*] Dr. T. Hasell, Dr. S. Y. Chong, Dr. M. Schmidtmann, Dr. D. J. Adams, Prof. A. I. Cooper
Department of Chemistry, Centre for Materials Discovery
University of Liverpool, Crown Street, Liverpool, L69 7ZD (UK)
E-mail: aicooper@liv.ac.uk

[**] We thank the EPSRC (grant number EP/H000925) and the University of Liverpool for funding, and Dr. K. E. Jelfs for suggestions and for producing Figure 4C. A.I.C. is a Royal Society Wolfson Merit Award holder.

Supporting information for this article is available on the WWW under http://dx.doi.org/10.1002/anie.201202849.

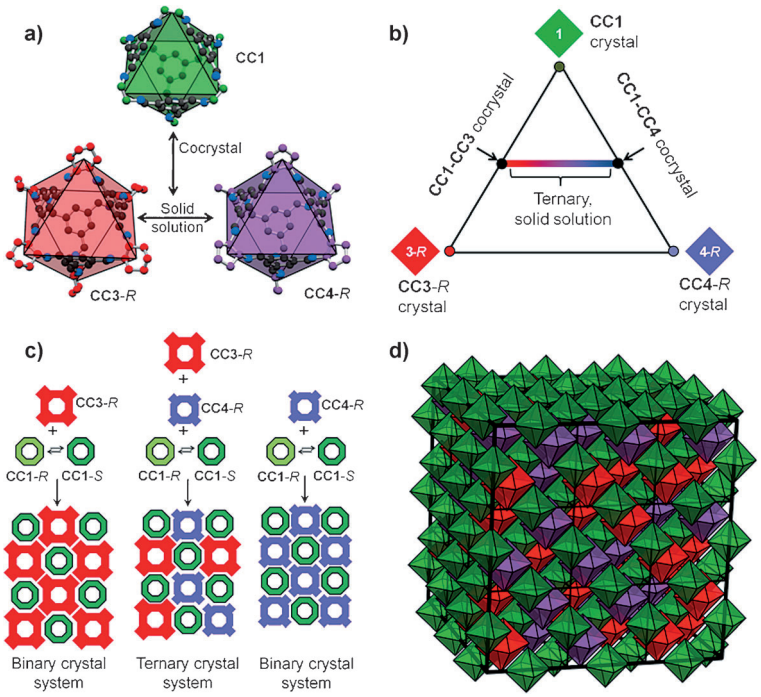

Figure 1. a) Structures of the three cage modules **CC1**, **CC3**-*R*, and **CC4**-*R*, which form a ternary cocrystal, b) where the *R* enantiomers comprise a solid solution. c) The chirality of **CC1** is resolved by cocrystallization with **CC3**-*R*, **CC4**-*R*, or a mixture of both modules. d) Cubic packing in the porous tercrystal. The **CC1** modules (green) occupy half of the lattice sites; **CC3**-*R* (red) and **CC4**-*R* (purple) are disordered over the remaining sites.

the Supporting Information). Hence, a broad range of relative compositions can be produced (Figure 1b).

Single-crystal X-ray diffraction analysis showed that the ternary cocrystals do assemble according to the intended scheme: that is, cage modules of opposite chirality interact much more favorably (Figure 1c,d). The ternary compositions, as well as the two binary cocrystals, **CC1**/**CC3**-*R* and **CC1**/**CC4**-*R*, all crystallize isostructurally in the cubic space group *F*23. **CC1**-*S* and **CC3**-*R*/**CC4**-*R* occupy alternating crystallographic positions, so that one half of the unit cell is occupied by **CC1** and the remainder by either **CC3** or **CC4** in the binary cocrystals, or a disordered solid solution of **CC3** and **CC4** in the ternary compositions. Each **CC1** cage is surrounded by four **CC3**/**CC4** cages in a window-to-window arrangement, and the principal feature of the diamondoid pore channel structure persists in all of the binary and ternary compositions discussed here. As per Scheme 1, there are no homochiral cage–cage interactions in the structures: each cage is surrounded by four cages of the opposite chirality. The cage composition in the solid state, as determined by X-ray diffraction, matches that present in solution to within 2%, as given in Table S1 (see the Supporting Information for crystallographic details).

These data show that **CC1**, **CC3**-*R*, and **CC4**-*R* combine to form a non-stoichiometric solid solution, or an "organic alloy",[2f,h] where **CC3** and **CC4** can be interchanged substitutionally into half of the sites of the cubic lattice. It is therefore possible to incorporate any relative ratio of the **CC3**-*R* and **CC4**-*R* modules without affecting the basic packing mode. This is markedly different from most molecular cocrystals, which tend to satisfy discrete molar ratios such as 1:1 or 2:1, and so on. This is, however, analogous with MTV-MOFs,[4] and the non-covalent chiral cage–cage pairing fulfills here a similar, dominant role to the extended metal–organic coordination bonds in the frameworks. One important difference, however, is that we do not observe a totally isotropic distribution of functionalities within the ternary cage cocrystals. Hence unlike the linkers in MTV-MOFs, only the **CC3**-*R* and **CC4**-*R* cages are disordered: the other half of the sites in the crystal are fully occupied by **CC1**.

Phase purity of the various cocrystal compositions was proved using powder X-ray diffraction (PXRD; Figure 2a), which also confirms a smooth transition in crystal properties as the ternary composition is varied.

Module **CC4** is smaller than **CC3**, being composed of cyclopentane rather than cyclohexane vertices. As a result, the unit cell dimensions of the ternary crystal, along with other physical properties, can be altered continuously by varying the ratio of **CC3**:**CC4**, as shown schematically in Figure 1c. In particular, small shifts of the diffraction peaks to higher angle demonstrate contraction of the unit cell as the proportion of **CC4**-*R* is increased (Figure 2b). This may stem from the smaller volume occupied by the **CC4**-*R* module in the structure or from closer cage packing because of more favorable interactions between **CC4**-*R* and the other modules, or from a combination of these two effects. The unit cell dimensions were extracted by Le Bail refinement of the PXRD pattern for each system and plotted as a function of the proportion of **CC4**-*R* (Figure 2c). This shows that the lattice parameters of the cocrystals decrease linearly with the incorporated proportion of **CC4**-*R*, as measured by NMR spectroscopy (Figure 2c), obeying Vegard's law,[8] and demonstrating that this system is functioning as an ideal solid solution. The lattice parameter, *a*, of the ternary crystal, **CC1**·**CC3**$_x$**CC4**$_{1-x}$, is given by Equation (1):

$$a_{\mathbf{CC1}\cdot\mathbf{CC3}_x\mathbf{CC4}_{1-x}} = x\, a_{\mathbf{CC1}\cdot\mathbf{CC3}} + (1\text{-}x) a_{\mathbf{CC1}\cdot\mathbf{CC4}} \quad (1)$$

Investigation of the cocrystals by scanning electron microscopy reveals geometric morphologies consistent with the crystal structures, and showed that the crystal habit changes across the compositional range (Figure 2d). Binary cocrystals of **CC1** and **CC3**-*R* form a rectified tetrahedron morphology, as does pure **CC3**-*R*. However, when a small proportion (12 mol%) of **CC4**-*R* is added, the crystals become truncated tetrahedra. For ternary cocrystals with equal proportions of **CC3**-*R* and **CC4**-*R*, the dominant morphology is tetrahedral crystals, combined with compound tetrahedra that form stellated octahedra (Figure 3). Binary cocrystals of **CC1** and **CC4**-*R* form tetrahedral crystals exclusively.

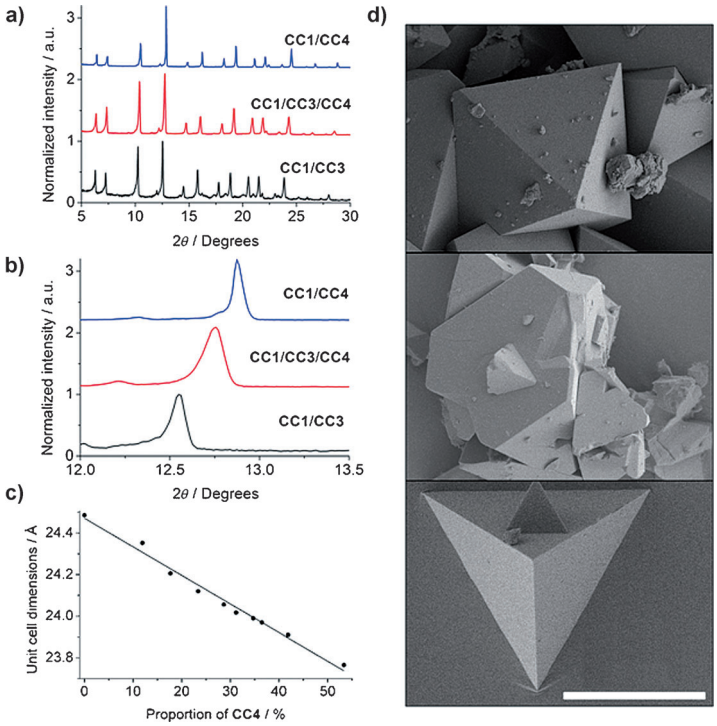

Figure 2. a) PXRD data for binary cocrystals and a 50:25:25 tercrystal of **CC1**, **CC3**, and **CC4**. b) Expansion showing a shift of diffraction peaks to higher angles as **CC4**-*R* proportion in the crystal is increased, resulting from a systematic decrease in the unit cell dimensions, as shown in (c). d) Electron micrographs showing evolution of crystal morphology for a binary **CC1**/**CC3**-*R* cocrystal (top; rectified tetrahedron), a 50:38:12 tercrystal of **CC1**, **CC3**, and **CC4** (middle; truncated tetrahedron), and a binary **CC1**/**CC4**-*R* cocrystal (bottom; tetrahedron). The scale bar is 10 μm.

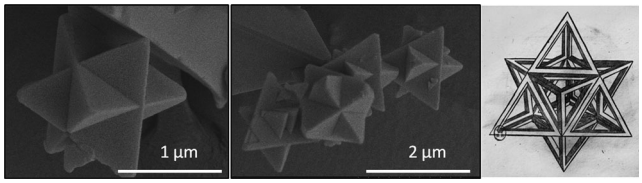

Figure 3. Electron micrographs of stellated octahedra in samples of **CC1**, **CC3**-*R*, and **CC4**-*R* ternary cocrystals. This shape, also known as a Stella Octangula, was depicted by Leonardo da Vinci in Pacioli's Divina Proportione in 1509 (image on the right).

The ability to continuously tune cocrystal composition raises, for the first time, the prospect of fine-tuning physical properties in porous organic cocrystals; for example, by using porous organic cages as "carrier modules" to position functionalities atomically with respect to one another. Here we give a preliminary example of such fine-tuning in terms of the gas sorption properties for the solids. All compositions gave rise to organic materials that were highly microporous as evidenced by gas sorption isotherms with classic type I shapes (Figure 4a).[11]

The samples produced with different **CC3**-*R*:**CC4**-*R* ratios showed apparent Brunauer–Emmett–Teller (BET) surface areas in the range of 373–670 $m^2 g^{-1}$, and nitrogen uptakes, as measured at $P/P_0 = 0.99$, 77.3 K, in the range 4.5–7.9 mmol g^{-1}. The relationship between the proportion of **CC4**-*R* and the surface area and the saturation nitrogen uptake are both close to linear (Figure 4b and Figure S2 in the Supporting Information). The surface area and nitrogen uptake for the binary **CC1**/**CC3**-*R* cocrystal is close to that observed for highly crystalline **CC3**-*R*,[9] which is broadly isostructural. The porosity can all be accounted for by the diamondoid pore channels shown in yellow in Figure 4c for the **CC1**/**CC4**-*R* analogue. However, as the proportion of **CC4**-*R* in the series of ternary crystals is increased, the gas uptake and surface area also increases. The binary **CC1**/**CC4**-*R* cocrystal adsorbs significantly more nitrogen than **CC1**/**CC3**-*R* or pure crystalline **CC3**-*R*,[8] and far too much to be accounted for by the diamondoid pore channel structure alone. We suggest that the additional microporosity in the **CC1**/**CC4**-*R* cocrystal stems from the interstitial voids (shown in orange in Figure 4c) that arise from the absence of bulky vertex groups on the **CC1** modules in the cocrystal. These interstitial voids have a volume that is large enough to account for the additional gas uptake. Although the voids are formally disconnected from the diamondoid pore channels, it is likely that they can be occupied by guests as a result of cooperative diffusion mechanisms, as observed for formally non-porous calixarenes.[12] This is further supported by the fact that the voids can be fully desolvated after the cocrystal synthesis, which involves removing solvent guests such as dichloromethane. This additional void volume does not seem to be expressed in terms of the nitrogen uptake for compositions with lower **CC4**-*R* contents; indeed, the quantity of N_2 adsorbed by the binary **CC1**/**CC3**-*R* cocrystals can be rationalized by the interconnected diamondoid channels alone. We speculate that the larger cyclohexane vertices in **CC1**/**CC3**-*R* could both constrict access to the occluded voids, and also inhibit dynamic movement in the crystal. The

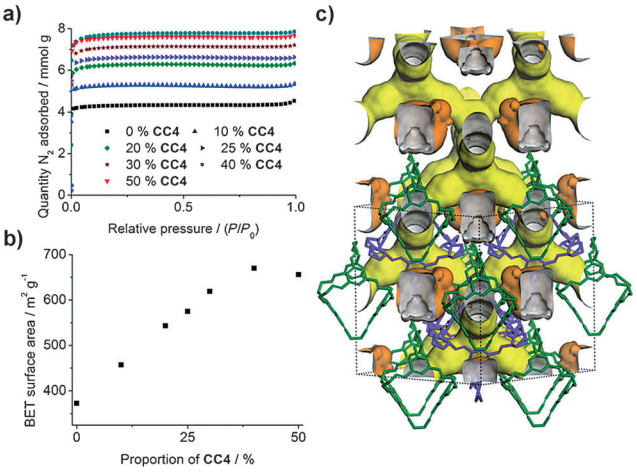

Figure 4. a) Nitrogen adsorption isotherms for cocrystals with various compositions measured at 77 K. b) Variation in apparent BET surface area as a function of cocrystal composition. c) Interconnected pore channels (yellow) and formally occluded interstitial voids (orange) in the **CC1**/**CC4**-*R* cocrystal.

discontinuity seen in Figure 3b in going from 40% to 50% **CC4**-*R* might stem from a counterbalancing increase in structural rigidity upon forming the pure binary **CC1**/**CC4**-*R* cocrystal.

In conclusion, understanding the interactions that occur between these porous molecules has made it possible to form a ternary crystal by design, rather than by chance, effectively treating the chiral cage pairing as a "bond" by analogy with isoreticular MOFs. **CC1** can be thought of as the "mortar" that holds together the two different types of "bricks" (**CC3**-*R* and **CC4**-*R*). There is no requirement for stoichiometric ratios of components, any ratio across a continuum may be used, leading to the first truly porous organic solid solution. Although the pore volumes here are relatively small, continuous fine-tuning of porosity as a function of composition may be useful, for example, in developing molecular separations. Also, the principle of specific positioning of cages within a ternary cocrystal might find applications in areas such as catalysis. Other studies[7c,d] demonstrate the possibility of chemically functionalizing the interior of porous organic cages. This suggests artificial enzyme mimics, where incompatible functionalities such as acids and bases are spatially positioned in a ternary cocrystal, the crystal packing being determined by the shape and functionality of the cage exterior.[6]

Experimental Section

Synthesis and cocrystallization: The three cage modules were synthesized as described previously.[9,13] Solutions of the cages were then prepared by dissolving each separately in dichloromethane (DCM) at a concentration of 4.47 mol L^{-1}. This corresponds to 5.00 mg mL^{-1} for **CC3**-*R*, 4.62 mg mL^{-1} for **CC4**-*R*, and 3.54 mg mL^{-1} for **CC1**. The solutions of **CC3**-*R* and **CC4**-*R* were mixed together first, in the appropriate proportions, and stirred to ensure homogeneous mixing. The required volume of **CC1** solution was then added to each sample. The solutions were added to glass vials which were then placed inside a glass tank containing acetone. The samples were left for three days to allow vapor diffusion to encourage crystallization. The crystals were then separated from the solvent by filtration. Characterization and crystallographic details are provided in the electronic Supporting Information. CCDC 876253, 876254, 876255, 876256 contains the supplementary crystallographic data for this paper. These data can be obtained free of charge from The Cambridge Crystallographic Data Centre via www.ccdc.cam.ac.uk/data_request/cif.

Received: April 13, 2012
Published online: June 8, 2012

Keywords: cocrystallization · crystal growth · organic alloys · porous organic cages · self-assembly

[1] A. D. Bond, *CrystEngComm* **2007**, *9*, 833 – 834.
[2] a) T. Smolka, R. Boese, R. Sustmann, *Struct. Chem.* **1999**, *10*, 429 – 431; b) C. B. Aakeröy, A. M. Beatty, B. A. Helfrich, *Angew. Chem.* **2001**, *113*, 3340; *Angew. Chem. Int. Ed.* **2001**, *40*, 3240; c) C. B. Aakeröy, J. Desper, M. M. Smith, *Chem. Commun.* **2007**, 3936 – 3938; d) B. R. Bhogala, S. Basavoju, A. Nangia, *Cryst. Growth Des.* **2005**, *5*, 1683 – 1686; e) L. H. Thomas, N. Blagden, M. J. Gutmann, A. A. Kallay, A. Parkin, C. C. Seaton, C. C. Wilson, *Cryst. Growth Des.* **2010**, *10*, 2770 – 2774; f) M. Dabros, P. R. Emery, V. R. Thalladi, *Angew. Chem.* **2007**, *119*, 4210 – 4213; *Angew. Chem. Int. Ed.* **2007**, *46*, 4132 – 4135; g) S. Tothadi, A. Mukherjee, G. R. Desiraju, *Chem. Commun.* **2011**, *47*, 12080 – 12082; h) R. Natarajan, G. Magro, L. N. Bridgland, A. Sirikulkajorn, S. Narayanan, L. E. Ryan, M. F. Haddow, A. G. Orpen, J. P. H. Charmant, A. J. Hudson, A. P. Davis, *Angew. Chem.* **2011**, *123*, 11588 – 11592; *Angew. Chem. Int. Ed.* **2011**, *50*, 11386 – 11390; i) K. Sada, K. Inoue, T. Tanaka, A. Epergyes, A. Tanaka, N. Tohnai, A. Matsumoto, M. Miyata, *Angew. Chem.* **2005**, *117*, 7221 – 7224; *Angew. Chem. Int. Ed.* **2005**, *44*, 7059 – 7062; j) A. I. Kitaigorodsky, *Mixed Crystals*, Springer, Heidelberg, **1984**.
[3] a) O. M. Yaghi, H. L. Li, C. Davis, D. Richardson, T. L. Groy, *Acc. Chem. Res.* **1998**, *31*, 474 – 484; b) A. K. Cheetham, G. Férey, T. Loiseau, *Angew. Chem.* **1999**, *111*, 3466 – 3492; *Angew. Chem. Int. Ed.* **1999**, *38*, 3268 – 3292; c) S. Kitagawa, R. Kitaura, S. Noro, *Angew. Chem.* **2004**, *116*, 2388 – 2430; *Angew. Chem. Int. Ed.* **2004**, *43*, 2334 – 2375.
[4] H. Deng, C. J. Doonan, H. Furukawa, R. B. Ferreira, J. Towne, C. B. Knobler, B. Wang, O. M. Yaghi, *Science* **2010**, *327*, 846 – 850.
[5] G. R. Desiraju, *Angew. Chem.* **2007**, *119*, 8492 – 8508; *Angew. Chem. Int. Ed.* **2007**, *46*, 8342 – 8356.
[6] M. Mastalerz, I. M. Oppel, *Angew. Chem.* **2012**, 124, 5345 – 5348; *Angew. Chem. Int. Ed.* **2012**, 51, 5252 – 5255.
[7] a) T. Tozawa, J. T. A. Jones, S. I. Swamy, S. Jiang, D. J. Adams, S. Shakespeare, R. Clowes, D. Bradshaw, T. Hasell, S. Y. Chong, C. Tang, S. Thompson, J. Parker, A. Trewin, J. Bacsa, A. M. Z. Slawin, A. Steiner, A. I. Cooper, *Nat. Mater.* **2009**, *8*, 973 – 978; b) J. T. A. Jones, T. Hasell, X. F. Wu, J. Bacsa, K. E. Jelfs, M. Schmidtmann, S. Y. Chong, D. J. Adams, A. Trewin, F. Schiffman, F. Cora, B. Slater, A. Steiner, G. M. Day, A. I. Cooper, *Nature* **2011**, *474*, 367 – 371; c) M. Mastalerz, M. W. Schneider, I. M. Oppel, O. Presly, *Angew. Chem.* **2011**, *123*, 1078 – 1083; *Angew. Chem. Int. Ed.* **2011**, *50*, 1046 – 1051; d) M. W. Schneider, I. M. Oppel, H. Ott, L. G. Lechner, H. J. S. Hauswald, R. Stoll, M. Mastalerz, *Chem. Eur. J.* **2012**, *18*, 836 – 847; e) J. Tian, P. K. Thallapally, B. P. McGrail, *CrystEngComm* **2012**, *14*, 1909 – 1919.
[8] L. Smart, E. A. Moore, *Solid State Chemistry: An Introduction*, Chapman & Hall, **1995**.
[9] T. Hasell, S. Y. Chong, K. E. Jelfs, D. J. Adams, A. I. Cooper, *J. Am. Chem. Soc.* **2012**, *134*, 588 – 598.
[10] T. Hasell, M. Schmidtmann, A. I. Cooper, *J. Am. Chem. Soc.* **2011**, *133*, 14920 – 14923.
[11] F. Rouquerol, J. Rouquerol, K. Sing, *Adsorption by Powders and Porous Solids*, Academic Press, San Diago, **1999**.
[12] J. L. Atwood, L. J. Barbour, A. Jerga, B. L. Schottel, *Science* **2002**, *298*, 1000 – 1002.
[13] a) T. Mitra, X. F. Wu, R. Clowes, J. T. A. Jones, K. E. Jelfs, D. J. Adams, A. Trewin, J. Bacsa, A. Steiner, A. I. Cooper, *Chem. Eur. J.* **2011**, *17*, 10235 – 10240; b) D. P. Lydon, N. L. Campbell, D. J. Adams, A. I. Cooper, *Synth. Commun.* **2011**, *41*, 2146 – 2151.

